Fatigue Cracking and Rutting Development in Secondary Road Pavements due to Wide-base Tire Loading

Hao Wang
Department of Civil Engineering, University of Illinois at Urbana-Champaign, Urbana, USA

Imad L. Al-Qadi
Department of Civil Engineering, University of Illinois at Urbana-Champaign, Urbana, USA

ABSTRACT: The main objective of this study is to evaluate the effect of new wide-base tires on secondary road pavements. A 3-D FE model was developed to predict pavement responses to loading applied by various tire configurations. The FE model incorporates measured 3-D tire-pavement contact stresses, modeled hot-mix asphalt (HMA) as linear viscoelastic, simulated continuous moving load, and utilizes implicit dynamic analysis. The analyzed pavement structures comprised of 76-mm HMA layer and aggregate base layer at various thicknesses (203, 305, 457 mm). The critical pavement responses under various tire configurations at intermediate and high temperatures were calculated and compared. The impact of wide-base tire 455 on fatigue cracking and rutting was analyzed using available damage models and compared to that resulted from conventional dual-tire assemblies. It was found that due to the different tire contact stress distributions, the wide-base 455 tire effects on secondary road pavements vary when compared to that of conventional dual-tire assembly. The wide-base 455 tire caused greater fatigue damage, subgrade rutting, and HMA rutting (densification), compared to the conventional dual-tire assembly when carrying the same load. On the other hand, the wide-base 455 tire causes less HMA rutting (shear) and base shear failure than the conventional dual-tire assembly. The damage ratios between the two tire configurations vary with various base thicknesses, temperatures, and possibly loading. The findings indicate that wide-base tires' impact on pavement damage on secondary roads depends on the roads' predominant failure mechanisms.

KEY WORDS: Wide-base tire, contact stress, fatigue cracking, rutting, secondary road.

1 INTRODUCTION

Managing the ever-increasing freight traffic is a challenge for the United States for several reasons. First of all, because trucks consume natural resources, including fuel, and contribute to gas emissions; they have a significant impact on the environment. In addition, the loading from heavy trucks accelerates pavement deterioration. Therefore, the US is in need of innovative technologies that can improve the efficiency of trucking operations while minimizing the damage to the environment and the road infrastructure.

One innovative technology is the use of wide-base single tires as an alternative to conventional dual-tire assemblies. Compared to conventional dual-tire assembly, wide-base tire offers the trucking industry significant economic advantages such as improved fuel efficiency, increased hauling capacity, reduced tire cost and repair, and superior ride and comfort. Wide-base tires also compare favorably to dual-tire assemblies with respect to truck operation and safety. With respect to environmental damage, the wide-base tires provide substantial benefits in gas emission reduction, noise reduction, and less tire material to recycle at the end of service life (Al-Qadi and Elsefi, 2007).

The first generation of wide-base tires (385/65R22.5 and 425/65R22.5) in the early 1980s were found to cause a significant increase in pavement damage compared to dual-tire assemblies. The new generation of wide-base tires (445/50R22.5 and 455/55R22.5) came to market in the 2000's in order to possibly reduce pavement damage and provide other safety and cost-saving advantages. The new generation of wide-base tires are 15 to 18% wider than the first generation and do not require high tire inflation pressure due to their special wall design (Al-Qadi et al. 2005). Results of COST Action 334 (2001) indicated that the new generation of wide-base tire would cause approximately the same primary rutting damage as a dual-tire assembly on primary roads and 44 to 52% more combined damage (20% primary rutting, 40% secondary rutting, and 40% fatigue cracking) on secondary roads. Al-Qadi et al. (2005) concluded that the new wide-base tires caused slightly more fatigue damage and less primary rutting damage than a dual-tire assembly, based on the studies conducted at the Virginia Smart Road. Priest et al. (2005) conducted a study at the NCAT Test Track in Auburn, Alabama and concluded that the new wide-base tire (445/50R22.5) resulted in a similar pavement fatigue life as the standard dual-tire assembly (275/80R22.5). The two aforementioned studies focused on conventional flexible pavements that are primarily used in the Interstate Highway System. Al-Qadi and Wang (2009) found that the new wide-base tire (455/55R22.5) induce greater fatigue damage but similar or less near-surface cracking and HMA rutting (shear flow) potential in full-depth asphalt pavements when compared to dual-tire assemblies.

The predominant failure mechanisms of secondary roads are different than those of primary roads or interstate highways. Although previous research has achieved significant advancements, it has not focused on the new wide-base tires' impact on secondary road pavements. Therefore, this study aimed to evaluate the pavement damage to secondary roads caused by the new wide-base tires.

2 OBJECTIVES AND SCOPE

The main objective of this study is to evaluate the effect of new wide-base tires on secondary road pavement; especially fatigue cracking and rutting. Previous research has attempted to use the linear layered elastic theory to predict pavement damage caused by various tire configurations (COST 334 2001). The layered theory assumes a uniform stress distribution within a circular contact area. However, this analytical technique cannot reflect the difference in contact stress distribution patterns between a wide-base tire and a conventional dual-tire assembly at tire-pavement interface. To overcome these limitations, a 3-D FE model was developed to simulate the realistic tire loading on secondary road pavements. The model allows for predicting pavement responses to loading applied by various tire configurations. It incorporates measured 3-D tire-pavement contact stresses, HMA linear viscoelasticity, continuous moving load, and utilizes implicit dynamic analysis.

The analyzed pavement structures were comprised of a 76-mm HMA layer and an unbound aggregate base layer at various thicknesses (203, 305, and 457mm). The critical pavement responses under various tire configurations at intermediate and high temperatures were calculated and compared. The impact of the new generation of wide-base tire (455/55R22.5) on secondary road pavement damage was compared to the impact of conventional dual-tire assembly for the aforementioned pavement designs.

3 DEVELOPMENT OF FINITE ELEMENT MODEL

The authors developed a 3-D FE model using ABAQUS version 6.7. A fine mesh was used around the loading area along the wheel path, and a relatively coarser mesh was used far away from the loading area. The element horizontal dimensions along the vehicle loading area were dictated by the tire rib and groove geometries. Hence, the length of elements within and around the loading area was selected at 15-18 mm in the transverse direction and 20 mm in the longitudinal (traffic) direction. The element thicknesses were selected at 10 mm for the upper HMA layers and 20-30 mm for the HMA base layers. Infinite elements were used at boundaries to reduce the otherwise large number of far-field elements without significant loss of accuracy and create "silent" boundaries for the dynamic analysis (ABAQUS 2007). The schematic illustration of the 3-D FE model is shown in Figure 1(a).

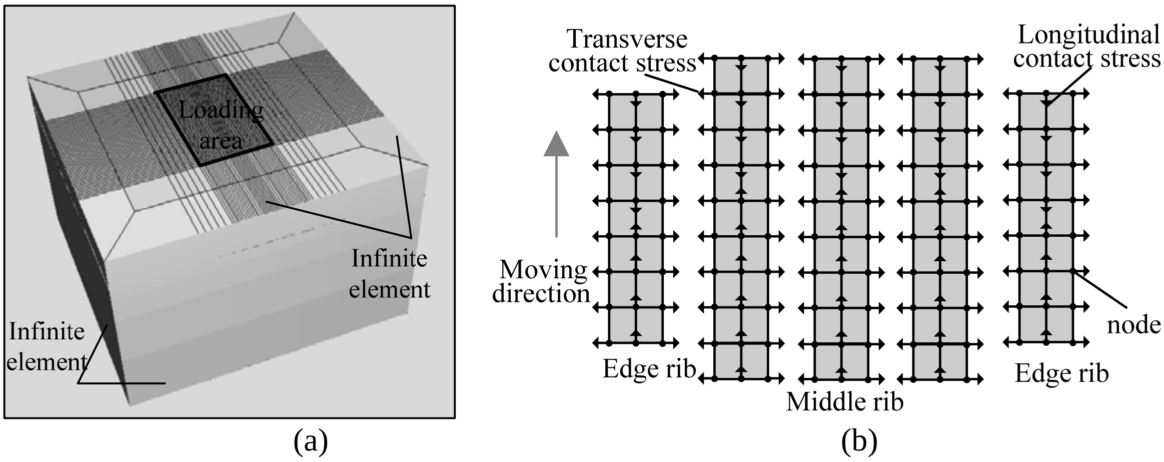

Figure 1: Schematic illustration of (a) 3-D FE model and (b) contact stresses under each rib of one tire

In the FE model, the measured 3-D tire-pavement contact stresses (vertical, transverse, and longitudinal) under each rib at free-rolling condition were applied on the tire imprint area, respectively (Figure 1(b)). These stresses were measured by tire manufacture at the flat pavement surface using triaxial load pins. Generally, the tire imprint area of each rib included two elements laterally and seven to ten elements longitudinally. The measured footprint shape at a specific load level and tire pressure was considered by adjusting the number and dimensions of elements within each rib. All elements along a tire rib were loaded with the non-uniform vertical contact stresses corresponding to their locations within the imprint area. The loading amplitudes of vertical contact stresses continuously change at each step as the tire is moving. The transverse and longitudinal contact stresses were converted into the equivalent concentrated forces using element shape functions and were assumed constant at each load step. The longitudinal contact stress was applied on the middle nodes of each rib, while the transverse contact stress was applied on the side nodes of each rib.

The dynamic transient pavement analysis was used in this study considering the inertia associated with the moving load and the dependency of the material properties on the loading frequency. The dynamic transient loading caused by a moving load is classified as a structure dynamics problem instead of a wave propagation problem, due to the fact that the vehicle speed is much less than the stress wave propagation speeds in the flexible pavement structure, 100 to 600 m/sec (OECD 1992). The dynamic equilibrium equation can be solved by a direct integration method such as implicit or explicit modes in ABAQUS. Using an implicit method is usually more effective for a structure dynamics problem such as this one. The energy dissipation rules among an arbitrary damping factor, a friction factor, or a viscoelastic material behavior can be defined in the dynamic analysis. In the case of using viscoelastic material behavior for the HMA layer, it is not necessary to introduce additional structural or mass damping rules for that layer. The damping ratio of 5% and the Rayleigh damping scheme were used for the subgrade and granular base layer (Chopra 2001).

Additional details about the 3-D FE model, tire contact stress, moving load simulation and dynamic transient analysis can be found in other literature. The model results have been validated using field strain measurements under truck loading as well as accelerated pavement testing (Yoo and Al-Qadi 2008, Al-Qadi et al. 2008, Wang and Al-Qadi 2009).

4 PAVEMETN STRUCTURE AND MATERIAL CHARACTERIZATION

The secondary road pavement structures used in this study resembled those constructed for accelerated pavement testing at the Advanced Transportation Research and Engineering Laboratory (ATREL) at the University of Illinois. More information on construction and instrumentation of these pavement sections can be found elsewhere (Al-Qadi et al. 2007). The analyzed pavement structures were comprised of 76-mm SM-9.5 (surface mix with maximum nominal aggregate size of 9.5mm) HMA layer and unbound aggregate base layer with various thicknesses (203, 305, and 457mm for sections A, B, and D, respectively). PG 64-22 binder was used in the SM-9.5 mix for the HMA layer. Dense-graded crushed limestone aggregates were used for the base layer. The pavement sections were constructed on subgrade with a low California Bearing Ratio (CBR) of 4%.

A linear viscoelastic model was used to simulate the HMA behavior. The HMA relaxation modulus was converted from laboratory determined creep compliance test results through an inter-conversion procedure (Park and Kim 1999). The shear and bulk relaxation moduli were then calculated, assuming a constant Poisson’s ratio, and fitted into a Prony series of generalized Maxwell solid model. The temperature dependency of HMA modulus was characterized by the time-temperature superposition principle because HMA has been proven as a thermo-rheologically simple (TRS) material. The time-temperature shift factor was approximated by the Williams-Landell-Ferry (WLF) function (ABAQUS 2007).

The aggregate base and subgrade were assumed as linear elastic material. The resilient modulus of subgrade was estimated from its CBR value using the approach in the 2002 Mechanistic-Empirical Pavement Design Guide (MEPDG) (ARA 2004). The resilient modulus of aggregate was estimated as the average measured modulus from repeated-load triaxial tests at five confining pressure levels (21, 35, 69, 104, and 138 kPa) following the AASHTO T307 procedure.

5 PAVEMENT DAMAGE ANALYSES

5.1 Pavement Damage Models

Generally, a pavement structure has three components: a HMA layer, granular or stabilized base/subbase layers, and subgrade. Each layer exhibits a unique mode of failure. The failure mode for each layer is related to that layer’s critical response at a specific position under loading. In this study, pavement damage models (also called transfer functions) were used to provide the relationship between the critical pavement responses and the allowed number of load applications before failure.

For a low-volume road with a thin HMA layer, the base layer plays an important role. In addition to the traditional design criteria of limiting the horizontal strain at the bottom of the HMA layer and the vertical compressive strain at the top of the subgrade, the permanent deformation of the base layer must also be considered. The accumulation of permanent deformation in the HMA layer may be caused by densification or shear flow or a combination of both. The main failure mechanisms in each pavement layer and the available damage models for flexible low-volume roads are summarized below.

<u>Fatigue Cracking</u>

Tensile strain at the bottom of the HMA layer is thought mainly responsible for bottom-up fatigue cracking. High tensile strains are usually caused by heavy load or the inadequate structural support from the underlying layers. The AASHTO 2002 MEPDG (ARA, 2004) determines the number of allowable load applications for fatigue cracking using Equation 1, where, N_f is number of allowed load applications; E is resilient modulus of HMA (in psi); ε_t is tensile strain at pavement surface; C is parameter related to HMA volumetric properties; and k is parameter related to HMA thickness. This method utilizes the initial pavement response and ignores the evolution of the strains with damage; however, the introduced error is considered acceptable within the empirical design framework.

$$N_f = 0.00432 \cdot k \cdot C \cdot (1/\varepsilon_t)^{3.9492} \left(1/E\right)^{1.281} \tag{1}$$

<u>HMA Rutting</u>

Two types of rutting (permanent deformation) may exist in a HMA layer simultaneously: volume reduction caused by traffic densification and aggregate particle movement with a constant volume or an increasing volume (dilation) caused by shear flow. The general form of HMA rutting models is usually derived from statistical analysis of the relationship between plastic and elastic compressive strains measured in the repeated-load uniaxial/triaxial test. The transfer function suggested by the AASHTO 2002 MEPDG (ARA, 2004) is shown in Equation 2, where, ε_p is accumulative permanent strain (12.5 mm rutting depth was used as failure criteria in this study); ε_r is recoverable strain; N is allowed number of load repetitions corresponding to ε_p; and T is pavement temperature (°C).

$$\log\left(\frac{\varepsilon_p}{\varepsilon_r}\right) = -3.7498 + 0.4262\log(N) + 2.02755\log(T) \tag{2}$$

Monismith et al. (1994) demonstrated that the accumulation of permanent deformation in the HMA layer was very sensitive to the layer’s resistance to shape distortion (i.e. shear) and relatively insensitive to volume change, especially under loading of slow moving vehicles at high temperature. Deacon et al. (2002) and Monismith et al. (2006) correlated HMA rutting to shear stresses and shear strains in the HMA layer instead of compressive strain, as shown in Equation 3, where, γ is permanent (inelastic) shear strain (12.5 mm rutting depth was used as failure criteria in this study); γ^e is elastic shear strain; τ_s is corresponding shear stress (in kPa); n is number of axle load applications; and a, b, and c are experimental determined coefficients (a=1.262, b=0.0072, c=0.36 were used in this study). This model was originally developed for Westrack mixes based on repeated simple shear test at constant height (RSST-CH).

$$\gamma = a \cdot \exp(b\tau_s)\gamma^e n^c \tag{3}$$

Permanent Deformation of Unbound Base Layer

Permanent deformation of the base layer is caused by the granular material having insufficient stability due to heavy loading or poor drainage conditions. This may result in loss of particle-to-particle interlock forces and thus the bearing capacity of base layer (shear failure). It is documented that the stress state in the middle of the unbound base layer indicates the development of deformation (Van Gurp and Van Leest, 2002). However, few design methods consider the cumulative permanent deformation or insufficient stability in granular base layer as critical.

In the South African Mechanistic Design Method (SA-MDM), the permanent deformation of the base layer is related to the ratio of the working stress to the yield strength of the material considering that high shear stress can extend into the base layer in thin-surfaced pavements for normal traffic loading (Theyse, 1996). Maree (1978) related the allowed load applications to the factor of safety by measuring the permanent deformation of granular material under dynamic triaxial loading, as shown in Equations 4 and 5, where, σ_1 and σ_3 are major and minor principal stresses (compressive stress positive and tensile stress negative); k is constant (k = 0.95 for normal moisture condition was used in this study); c is cohesion coefficient; ϕ is angle of internal friction (c=0, ϕ=30^{o} were used in this study); and N is allowed load applications until failure. The safety factor concept was developed from the Mohr-Coulomb theory and represents the ratio of the material shear strength divided by the applied deviator stress.

$$F = \frac{\sigma_3[k(\tan^2(45+\frac{\phi}{2})-1] + 2kc\tan(45+\frac{\phi}{2})}{\sigma_1 - \sigma_3} \tag{4}$$

$$N = 10^{(2.605122F + 3.480098)} \tag{5}$$

Subgrade Rutting

Subgrade rutting (secondary rutting) is a longitudinal wheel-path depression that occurs when subgrade exhibits permanent deformation caused by compressive or shear stresses due to repetitive traffic loading. Usually, the vertical compressive strain at the top of the subgrade is related to subgrade rutting. The Asphalt Institute (1982) proposed a rutting damage model based on roadbed soil vertical compressive strain with the maximum threshold of 12.5 mm rutting on subgrade (Equation 6), where, N is allowed load repetitions until failure, and ε_v is maximum vertical compressive strain on top of subgrade.

$$N = 1.365 \times 10^{-9} (\varepsilon_v)^{-4.477} \tag{6}$$

5.2 Damage Ratio between Two Tire Configurations

Using the calculated pavement responses from the FE model and the aforementioned damage models, Tables 1 through 3 present the calculated damage ratios caused by the 455 wide-base tire with respect to the dual-tire assembly (35.5 kN, 690 kPa, 8 km/h), respectively, for bottom-up fatigue cracking, HMA rutting caused by densification and shape distortion. Tables 4 and 5 presented the damage ratios in the unbound granular base and subgrade, respectively. The damage ratio for each specific failure mechanism was calculated using Equation 7, where, DR is damage ratio caused by the 455 wide-base tire with respect to the dual-tire assembly for the considered failure mechanism; N_{w455} is allowable number of load applications to failure for the 455 wide-base tire; and N_{dual} is allowable number of load applications to failure for dual-tire assembly. For fatigue cracking, shear failure, and secondary rutting, the allowable number of load applications to failure can be directly predicted from Equations 1, 5, and 6, respectively. For HMA rutting caused by densification and shear, the damage ratio is calculated as the ratio of the required load applications of the dual tire assembly to that of wide base tire to achieve the same plastic strain (Equations 2 and 3).

$$DR = N_{dual} / N_{w455} \tag{7}$$

The results show that the 455 wide-base tire causes greater fatigue damage, subgrade rutting and HMA rutting (densification) compared to the conventional dual-tire assembly. For subgrade rutting and HMA rutting due to densification, the relative damage ratios between the two tire configurations decrease as the base thickness increases. On the other hand, the wide-base 455 tire causes much less HMA rutting due to shear flow than the conventional dual-tire assembly, especially at high temperature. It is noted that for the base shear failure the wide-base 455 tire causes greater deviator stress, which increases the failure potential, but it also causes greater confinement stress, which restricts shear failure. The ratio of confinement stress with respect to deviator stress in the base layer is greater under a 455 wide-base tire than under a dual-tire assembly. This reduces the relative potential of shear failure in the unbound base layer.

The damage ratio can be used to convert the number of axles with wide-base tires to the number of axles with dual-tire assembly in pavement design practice. If the pavement is designed based on a specific failure type using a mechanistic-empirical approach, the damage ratio corresponding to the specific failure mechanism can be used. If the pavement is designed following the AASHTO design procedure (AASHTO, 1993), the load equivalent factor (LEF) for the corresponding wide-base tires can be calculated as: LEF for wide-base tires at a given axle load is equal to AASHTO LEF for the axle load multiplied by the damage ratio obtained from this study .

Table 1 Damage ratios for bottom-up fatigue cracking between two tire configurations

Temperature (^{o}C)	Base thickness (mm)	Critical tensile strains (micro)		Damage ratio
		Dual	Wide-base	
25	203	331	403	2.18
	305	297	364	2.23
	457	248	310	2.41
47	203	1005	1232	2.24
	305	945	1113	1.91
	457	750	946	2.50

Table 2 Damage ratios for HMA rutting (densification) between two tire configurations

Temperature (°C)	Base thickness (mm)	Critical compressive strains (micro)		Damage ratio
		Dual	Wide-base	
25	203	355	453	1.77
	305	324	412	1.76
	457	272	345	1.75
47	203	1520	1820	1.53
	305	1430	1690	1.48
	457	1240	1410	1.35

Table 3 Damage ratios for HMA rutting (shear) between two tire configurations

Temperature (°C)	Base thickness (mm)	Critical shear strains (micro)		Critical shear stress (kPa)		Damage ratio
		Dual	Wide-base	Dual	Wide-base	
25	203	255	259	409	400	0.81
	305	243	244	397	384	0.68
	457	230	222	380	358	0.43
47	203	1389	1212	306	259	0.27
	305	1342	1124	300	249	0.22
	457	1342	1124	298	248	0.22

Table 4 Damage ratios for base shear failure between two tire configurations

Temperature (°C)	Base thickness (mm)	Deviator stress (kPa)		Minor principal stress (kPa)		Damage ratio
		Dual	Wide-base	Dual	Wide-base	
25	203	84	112	39	53	0.69
	305	66	111	30	40	0.92
	457	42	103	9	12	0.96
47	203	169	217	57	76	0.87
	305	158	214	35	49	0.92
	457	122	164	6	9	0.94

Table 5 Damage ratios for subgrade rutting between two tire configurations

Temperature (°C)	Base thickness (mm)	Critical subgrade compressive strains (micro)		Damage ratio
		Dual	Wide-base	
25	203	1347	1510	1.67

	305	1134	1205	1.31
	457	770	818	1.31
	203	1660	2010	2.35
47	305	1283	1414	1.55
	457	801	856	1.35

6 CONCLUSIONS

In this study, a three-dimensional (3-D) finite element model is developed to predict pavement responses to loading applied by various tire configurations on secondary road pavements. The effect of wide-base tires on HMA fatigue cracking and rutting was analyzed using available damage models, and the results were compared to the damage from conventional dual-tire assemblies. The results show that the new generation of wide-base tire causes greater fatigue damage, subgrade rutting, and HMA rutting (densification) compared to the conventional dual-tire assembly when carrying the same load on secondary road. On the other hand, the new wide-base tire causes less HMA rutting (shear) and base shear failure potential than the conventional dual-tire assembly. These damage ratios vary with base layer thicknesses, temperatures, and possibly loading. The findings indicate that wide-base tires' damage impact on secondary road pavements depends on the roads' predominant failure mechanisms.

REFERENCES

AASHTO (1993). AASHTO Guide for design of pavement structures. American Association of State Highway and Transportation Officials (AASHTO), Washington D.C.

ABAQUS (2007). ABAQUS/Standard User's Manual Version 6.7, Hibbitt, Karlsson & Sorenson, Inc., Pawtucket, RI.

Al-Qadi, I.L., P.J. Yoo, M.A. Elseifi, and I. Janajreh (2005). Effects of Tire Configurations on Pavement Damage, Journal of the Association of Asphalt Paving Technologists, Vol. 74, p. 921-962.

Al-Qadi, I.L. and M.A. Elseifi (2007). State-of-the-Practice of the New Generation of Wide-Base Tire and its Impact on Trucking Operations, Transportation Research Record, 2008, TRB, Washington, D.C., p. 100-109.

Al-Qadi, I.L., E. Tutumluer, S.H. Dessouky, and J. Kwon (2007). Effectiveness of Geogrid-Reinforcement in Flexible Pavements: A Full-Scale Testing, Final Report to Tensar Earth Technologies, Inc., University of Illinois at Urbana-Champaign.

Al-Qadi I.L., H. Wang, P.J. Yoo, and S.H. Dessouky (2008). Dynamic Analysis and In-situ Validation of Perpetual Pavement Response to Vehicular Loading, Transportation Research Record, 2087, p. 29-39.

Al-Qadi, I.L., and H. Wang (2009). Full-depth Pavement Responses under Various Tire Configurations: Accelerated Pavement Testing and Finite Element Modeling, accepted by the Journal of the Association of Asphalt Paving Technologists, Vol. 78, p. 645-680.

ARA, Inc. (2004). ERES Division, Development of the 2002 Guide for the Design of New and Rehabilitated Pavements, NCHRP 1-37A, Transportation Research Board, Washington, D.C.

Asphalt Institute (1982). Research and Development of the Asphalt Institute's Thickness Design Manual (MS-1), Research report 82-1, 9th ed., College Park, MD.

Bathe, K.J. (1982). Finite Element Procedures in Engineering Analysis, Prentice-Hall, NJ.

Chopra, A.K. (2001). Dynamics of Structures, 2nd ed., Prentice Hall, Upper Saddle River, NJ.

COST 334 (2001). Effects of Wide Single Tires and Dual Tires, Final report of the action, European Cooperation in the Field of Scientific and Technical Research, Brussels, Belgium.

Deacon J.A., J.T. Harvey, I. Guada, L. Popescu, and C.L. Monismith, (2002). Analytically Based Approach to Rutting Prediction, Transportation Research Record, 1806, p. 9-18.

Maree, J.H. (1978). Design Parameters for Crushed Stone in Pavements, M. Eng thesis, Department of Civil Engineering, Faculty of Engineering, University of Pretoria, South Africa.

Monismith C.L., R.G. Hicks, F.N. Finn, J. Sousa, J. Harvey, S. Weissman, J. Deacon, J. Coplantz, and G. Paulsen (1994). Permanent Deformation Response of Asphalt Aggregate Mix, SHRP-A-415 Report, Strategic Highway Research Program, National Research Council, Washington, D.C.

Monismith C.L., L. Popescu, and J.T. Harvey (2006). Rut Depth Estimation for Mechanistic-Empirical Pavement Design Using Simple Shear Test Results, Journal of Association of Asphalt Paving Technologists, Vol.75.

Organization for Economic Co-Operation and Development (1992). Dynamic Loading of Pavements, OECD report, OECD, Paris, France.

Park, S.W. and Y. R. Kim (1999). Interconversion between Relaxation Modulus and Creep Compliance for Viscoelastic Solids. ASCE Journal of Materials in Civil Engineering, Vol. 11, No. 1, pp. 76–82.

Priest, A.L., D.H. Timm, and W.E. Barrett (2005). Mechanistic Comparison of Wide-base Single vs. Standard Dual Tire Configurations, Final Report, National Center for Asphalt Technology (NCAT), Auburn, AL.

Theyse, H.L., M. De Beer, and F.C. Rust (1996). Overview of the South African Mechanistic Pavement Design Analysis Method, Transportation Research Record, 1539, p. 6-17.

Van Gurp, C, and A.J. Van Leest, (2002). Thin Asphalt Pavements on Soft Soil, Proc. 9th International Conference on Asphalt Pavements, International Society for Asphalt Pavements, Copenhagen, Denmark.

Wang, H. and I.L. Al-Qadi (2009). Combined Effect of Moving Wheel Loading and Three-Dimensional Contact Stresses on Perpetual Pavement Responses, Transportation Research Record, 2095, p. 53-61.

Yoo, P.J. and I.L. Al-Qadi (2008). Truth and Myth of Fatigue Cracking Potential in Hot-Mix Asphalt: Numerical Analysis and Validation, Journal of Association of Asphalt Paving Technologists, vol. 77, p. 549-590.